

## Ferromagnetic-induced component in piezoresistance of GaMnAs

K. Onomitsu, I. Mahboob, H. Okamoto, Y. Krockenberger, and H. Yamaguchi

*NTT Basic Research Laboratories, NTT Corporation, 3-1 Morinosato-Wakamiya, Atsugi, Kanagawa 243-0198, Japan*

(Received 13 June 2011; revised manuscript received 13 July 2012; published 28 February 2013)

We have observed a ferromagnetic-induced piezoresistance component in a micromechanical cantilever integrated with a GaMnAs piezoresistor. The temperature and the magnetic-field dependence of the piezoresistance around the ferromagnetic transition reveal that the piezoresistance is modulated by ferromagnetic ordering. The sign of the ferromagnetic-induced component of the piezoresistance is opposite to that of the conventional piezoresistance, though of comparable magnitude. This ferromagnetic-induced piezoresistance has a delayed response to mechanically induced strain, with an experimentally determined response time of  $230 \pm 35$  ns.

DOI: [10.1103/PhysRevB.87.060410](https://doi.org/10.1103/PhysRevB.87.060410)

PACS number(s): 75.50.Pp, 72.20.Fr, 75.78.-n, 85.85.+j

The piezoresistive effect (PR) is defined as the change in resistance of a material due to an applied stress and is a fundamental property of semiconductors and metals.<sup>1-9</sup> In conventional semiconductors, PR originates from a change in either carrier density or mobility. PR can also be observed in metals, including ferromagnetic materials, due to geometrical effects.<sup>7-9</sup> PR provides a powerful tool for the investigation of electronic transport properties and can be used for sensing applications.<sup>10-14</sup> Here we report a mechanism of PR in GaMnAs where the ferromagnetic ordering plays an essential role. We characterized PR by incorporating a GaMnAs piezoresistor into a micromechanical cantilever<sup>13,14</sup> and investigated its temperature and magnetic-field dependence at the ferromagnetic transition. A clear ferromagnetic-induced piezoresistance (FM-PR) component was found below the Curie temperature ( $T_c$ ) of our GaMnAs ( $T_c \approx 48$  K). Our results indicate that the FM-PR of GaMnAs arises from the perturbation of spontaneous spin ordering by the applied strain. Moreover, the change in resistance is delayed with respect to mechanical strain. We deduced a delay time of  $230 \pm 35$  ns. The experimental results presented here indicate that the micromechanical method of characterizing spin dynamics is complementary to conventional electrical and optical methods.<sup>15-19</sup>

A 100-nm-thick GaMnAs layer was heteroepitaxially grown on a semi-insulating GaAs(001) substrate [Fig. 1(a)]. The growth was performed by migration-enhanced epitaxy<sup>20</sup> to avoid both MnAs precipitates and excess As. Secondary ion mass spectrometry (SIMS) revealed the Mn content to be  $\sim 1\%$ . Magnetization measurements were performed using a superconducting quantum interference device (SQUID). The  $T_c$  of our GaMnAs layer is 48 K, similar to other reports.<sup>21</sup> Data obtained from magnetoresistance and Hall measurements of our GaMnAs sample are similar to reported ones for compressively strained GaMnAs film.<sup>22,23</sup> The easy axes of magnetization are in-plane oriented for compressively strained films; so, the direction orthogonal to the wafer surface is parallel to the magnetic hard axis. Our GaMnAs wafer was processed into a 200- $\mu\text{m}$ -long, 60- $\mu\text{m}$ -wide cantilever with a thickness of 4.1  $\mu\text{m}$  [Fig. 1(b)] by the standard micro-machining technique where the  $\text{Al}_{0.7}\text{Ga}_{0.3}\text{As}$  sacrificial layer was etched. A 1- $\mu\text{m}$ -thick  $\text{Al}_{0.25}\text{Ga}_{0.75}\text{As}$  strain compensation layer was inserted below the GaAs in order to prevent the inherent deflection of the cantilever owing to the lattice mismatch

between GaMnAs and GaAs. A conductive channel of GaMnAs was formed on the cantilever for the measurement of the PR, i.e., the variation of the two-terminal resistance of the channel subject to mechanical resonance. Residual GaMnAs film material around the channel area was etched in order to minimize the influence of the magnetization related torque on the resonance frequency.<sup>13</sup> The cantilever was mounted on piezoceramic crystal  $\text{Pb}(\text{Zr-Ti})\text{O}_3$  and actuated by applying an ac voltage. When the actuation frequency is swept, the cantilever resonates at the fundamental-mode frequency ( $f_0$ ), and the frequency response is electrically detected by measuring the PR. The mechanical  $Q$  is 21 000 at 55 K, i.e., above  $T_c$ . We employed a frequency-mixing technique, where the bias-current ( $f_1$ ), actuation ( $f_2$ ), and reference frequencies ( $f_1 - f_2$ ) are different,<sup>14,24,25</sup> as shown in Fig. 1(b). It is well known that capacitive and inductive components tend to generate superpositions in electrical circuits. The mixing technique can minimize such capacitive and inductive crosstalk. In order to rule out the existence of crosstalk in our experimental setup, the PR experiments have been performed with various mixing frequencies ( $f_1 - f_2$ ), different measurement setups, as well as different cantilever geometries. Our results unambiguously show that the obtained data solely originate from the device's PR response. The PR characterization was performed under a magnetic field along the [001] direction, parallel to the magnetic hard axis. All PR measurements were carried out under vacuum since ambient conditions broaden the resonance peak.

The zero-magnetic field PR<sup>26</sup> around  $f_0$  was measured with a lock-in amplifier. We plotted the real [Fig. 2(a)] and imaginary [Fig. 2(b)] parts of the change of the two-terminal resistance relative to its actuation frequency for various temperatures. In general, a displacement of a harmonic oscillator has a frequency response where the real part is given by a symmetric function and the imaginary part by an asymmetric function. Such frequency dependence corresponds to a response delay of  $\pi/2$  in the real part and  $\pi$  in the imaginary part with respect to a sinusoidal actuation force. This behavior reflects the delay in the cantilever response; the phase difference between the applied force and the displacement changes continuously from 0 to  $\pi$  as the actuation frequency is swept across  $f_0$ , which is common to damped harmonic oscillators.<sup>27</sup> (We can observe the frequency response by measuring the PR, since PR is proportional to the displacement.)

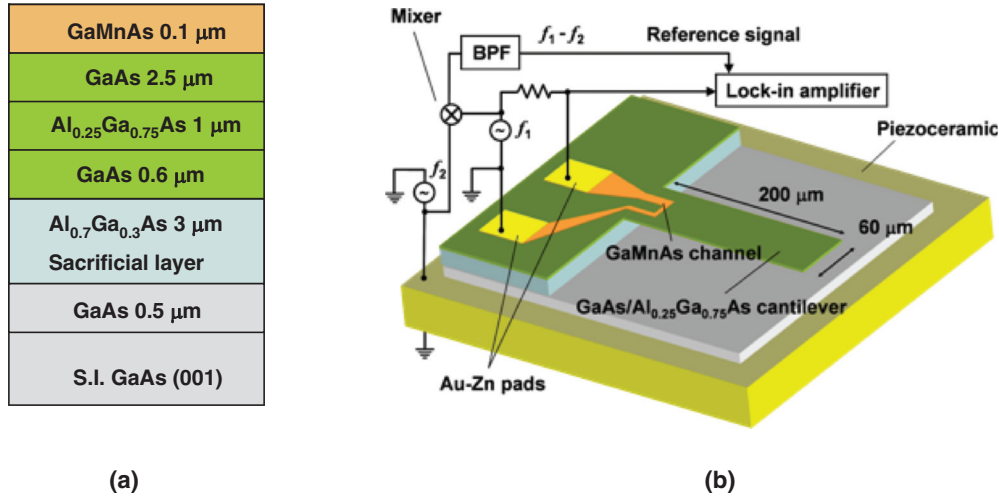


FIG. 1. (Color online) Schematics of the structure of the cantilever together with experimental setup. (a) Cross-sectional view of the layers of the cantilever. Each layer was grown by molecular beam epitaxy. The cantilever consists of a 100-nm-thick GaMnAs layer, a 2.5- $\mu\text{m}$ -thick GaAs layer, and an  $\text{Al}_{0.25}\text{Ga}_{0.75}\text{As}$  layer which is a strain compensation layer and 0.6  $\mu\text{m}$  thick. Below the cantilever layer, a 3- $\mu\text{m}$ -thick  $\text{Al}_{0.7}\text{Ga}_{0.3}\text{As}$  sacrificial layer has been inserted and selectively etched by HF. (b) Schematic illustration of the cantilever together with electrode on piezoelectric transducer and measurements setup. The frequency response of PR is detected via down-mixing technique. The reference frequency can be tuned by adjusting bias-current frequency ( $f_1$ ) and actuation frequency ( $f_2$ ).

Well above  $T_c$  ( $T > 50$  K), the magnitude of the PR, i.e., its peak height, shows a weak temperature dependence, which is similar to that of diamagnetic GaAs (not shown). In contrast, the PR changes abruptly below  $T_c$ : Lowering the temperature initially reduces the magnitude of the PR and then increases it with the opposite sign. This behavior is not observed in diamagnetic GaAs. Thus, an additional PR component is induced with the opposite sign due to the ferromagnetic ordering. The strong correlation between spontaneous ferromagnetic ordering and the PR component was also observed when the magnetic field was applied perpendicular to the substrate surface. The magnetic moment is polarized by an external magnetic field along the magnetic hard axis. Thus, the spontaneous in-plane spin ordering is rotated and the additional PR component is suppressed by the applied magnetic field. The real part of the frequency response was measured as a function of magnetic field ( $B$ ) at various temperatures (Fig. 3). At 55 K [Fig. 3(a)], which is well above  $T_c$ , the PR shows no  $B$  dependence. Thus, the PR above  $T_c$  is of nonferromagnetic origin. However, below  $T_c$ , PR exhibits a strong  $B$  dependence both in magnitude and resonance frequency. For instance, at 40 K [Fig. 3(c)], the dependence of the magnitude of the PR on magnetic field is similar to that on the temperature: Increasing the magnetic field initially reduces the magnitude of the PR followed by an increase, though with the opposite sign. A continuous variation from 55 to 35 K [Figs. 3(a)–3(d)] indicates that a common mechanism causes the additional PR component, both in the temperature and magnetic-field dependence.

The PR ( $\Pi$ ) of GaMnAs can be modeled by the sum of FMPR ( $\Pi_{\text{FM}}$ ) and a nonferromagnetic component ( $\Pi_0$ ):  $\Pi = \Pi_{\text{FM}}(\sigma) + \Pi_0$ . Here,  $\Pi_{\text{FM}}$  has a sign opposite to  $\Pi_0$  and strongly depends on the degree of spontaneous in-plane spin ordering ( $\sigma$ ). When the spontaneous spin ordering appears as a result of reducing either the temperature or the applied magnetic field, the magnitude of  $\Pi_{\text{FM}}$  increases. The compensation

temperature  $T_{\text{comp}}$  is defined when  $|\Pi_{\text{FM}}(\sigma)| = |\Pi_0|$ . Between  $T_c$  and  $T_{\text{comp}}$ ,  $\Pi$  thus becomes monotonically smaller with decreasing temperature. Further decreasing the temperature results in a sign reversion of  $\Pi$  due to increasing  $\Pi_{\text{FM}}$ . It is worth noting that both contributions do not completely compensate each other, even when their magnitudes are equal. For example, the real and imaginary parts of the PR (Fig. 2) change from symmetric/antisymmetric (S/AS) behavior to AS/S behavior at the compensation temperature ( $T_{\text{comp}} \approx 44$  K). A similar behavior was also observed in the magnetic-field dependence at lower temperatures. Such imperfect compensation phenomenon can be explained by assuming that the response of FMPR to strain is delayed, as we discuss below.

The strain induced mechanically in a GaMnAs piezoresistor is proportional to the displacement of the cantilever in the linear elastic regime. If we assume that the FMPR has a delay with a time constant  $\tau$  in response to mechanically induced strain, then  $\Pi_0$  and  $\Pi_{\text{FM}}$  can be written as

$$\Pi_0(t) = C_0 x(t), \quad \Pi_{\text{FM}}(t) = C_{\text{FM}}(\sigma) \int_{-\infty}^t dt' e^{-(t-t')/\tau} x(t')/\tau, \quad (1)$$

where  $C_0$  and  $C_{\text{FM}}(\sigma)$  are the piezoresistive coupling constants and  $x(t)$  is the displacement of the cantilever at time  $t$ . We assume that the response of  $\Pi_0$  is much faster than the movement of the cantilever because the deformation of the band structure is the origin of  $\Pi_0$ . At 50 K ( $>T_c$ ), the measured PR is simply given by  $\Pi_0$ . Below  $T_c$ ,  $C_{\text{FM}}(\sigma)$  becomes finite with the opposite sign and terminates  $\Pi_0$ . In the small- $\tau$  limit, the two contributions completely compensate at  $T_{\text{comp}}$ . However, if  $2\pi f_0 \tau$  is large enough to be detectable with the used measurement setup ( $>0.01$  in our case), a total compensation is not observed. The oscillation of the cantilever

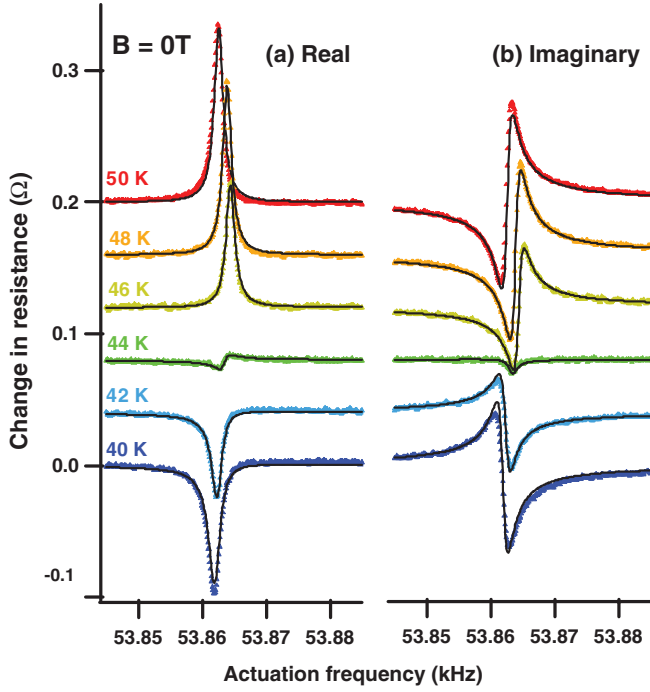


FIG. 2. (Color online) Temperature dependence of PR around  $T_c$  without external magnetic field: (a) real part and (b) imaginary part. Data (colored dots) show the measured frequency response, and the straight lines (black) were obtained using Eqs. (3)–(6) with  $\tau = 230$  ns obtained at  $T_{\text{comp}} = 44$  K. Data and calculated lines have been offset by  $\Delta = 0.04 \Omega$  for clarity.

is given by the following equation of a harmonic oscillator:

$$m\ddot{x}(t) + (m\omega_0/Q)\dot{x}(t) + m\omega_0^2x(t) = F_0 \sin \omega t, \quad (2)$$

where  $\omega_0 = 2\pi f_0$ ,  $Q$  is the quality factor,  $F_0$  is the amplitude of the driving force, and  $m$  is the effective mass of the cantilever. From Eqs. (1) and (2), we obtain

$$\Pi(t) = R(\omega) \cos \omega t + I(\omega) \sin \omega t, \quad (3)$$

$$R(\omega) = C_0 f(\omega) + C_{\text{FM}} \{f(\omega) - \tau \omega g(\omega)\} / \{(\tau \omega)^2 + 1\}, \quad (4)$$

$$I(\omega) = C_0 g(\omega) + C_{\text{FM}} \{g(\omega) + \tau \omega f(\omega)\} / \{(\tau \omega)^2 + 1\}, \quad (5)$$

$$f(\omega) = \frac{F_0 \omega_0 \omega / m Q}{(\omega^2 - \omega_0^2)^2 + \omega^2 \omega_0^2 / Q^2},$$

$$g(\omega) = \frac{F_0 (\omega^2 - \omega_0^2) / m}{(\omega^2 - \omega_0^2)^2 + \omega^2 \omega_0^2 / Q^2}. \quad (6)$$

The coefficients  $R(\omega)$  and  $I(\omega)$  correspond to the real and imaginary parts obtained from the lock-in amplifier. Since  $R(\omega)$  is an asymmetric function of  $\omega$  at the compensation temperature ( $T_{\text{comp}} = 44$  K), from Eqs. (4) and (6) we obtain

$$C_{\text{FM}} = -C_0 \{(\tau \omega_0)^2 + 1\}. \quad (7)$$

Applying this condition, we obtain an approximate expression for PR at the  $T_{\text{comp}}$ :

$$\Pi(t) \approx \tau \omega C_0 \{g(\omega) \cos \omega t - f(\omega) \sin \omega t\}. \quad (8)$$

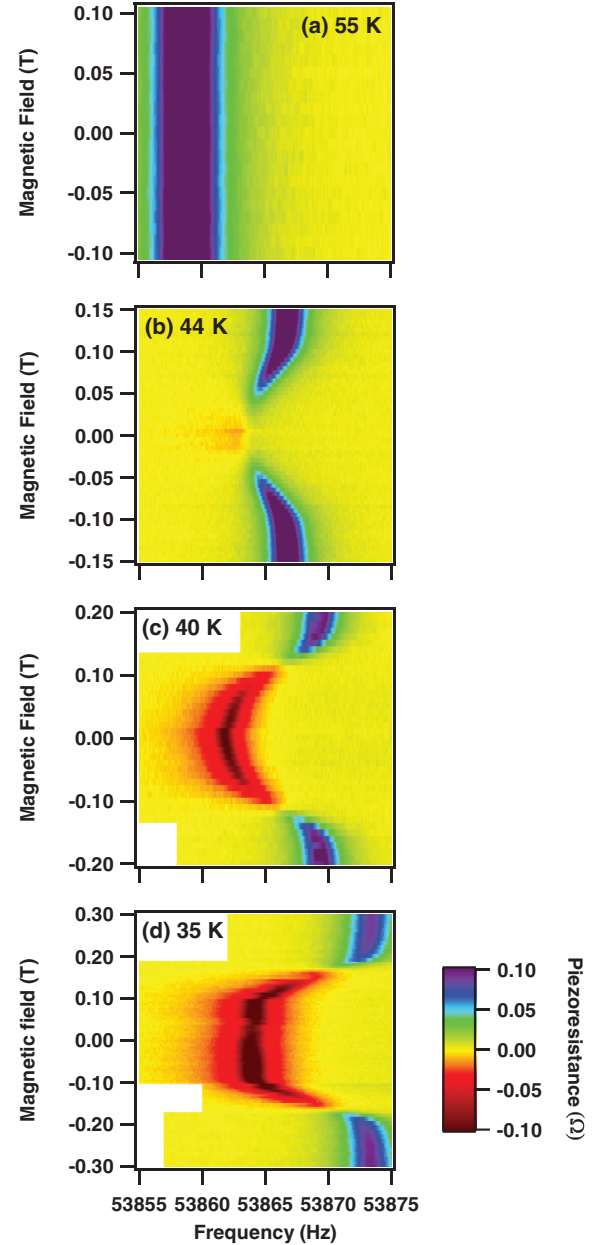


FIG. 3. (Color online) The real part of PR was measured at various temperatures [(a) 55, (b) 44, (c) 40, and (d) 35 K] under external magnetic field. The magnetic field is applied perpendicular to the sample surface (parallel to magnetic hard axis). Above  $T_c$  (48 K), PR does not depend on  $B$  (a). Below  $T_c$ , PR shows a phase rotation [(b), (c), and (d)] with magnetic field strength and polarity.

In contrast, the nonferromagnetic component is given by

$$\Pi_0(t) = C_0 \{f(\omega) \cos \omega t + g(\omega) \sin \omega t\}. \quad (9)$$

Equations (8) and (9) well explain our experimental results at the  $T_{\text{comp}}$  where the phase of the PR is rotated by  $\pi/2$  with respect to that above  $T_c$ . If we assume that  $C_0$  has a negligible temperature dependence around  $T_c$ , we obtain a delay time of  $\tau = 230 \pm 35$  ns by fitting Eqs. (3)–(6) to the data in Fig. 2. Our fitting results show very good agreement with the experimentally obtained curves in Fig. 2. Here, we emphasize again that a similar delay time was

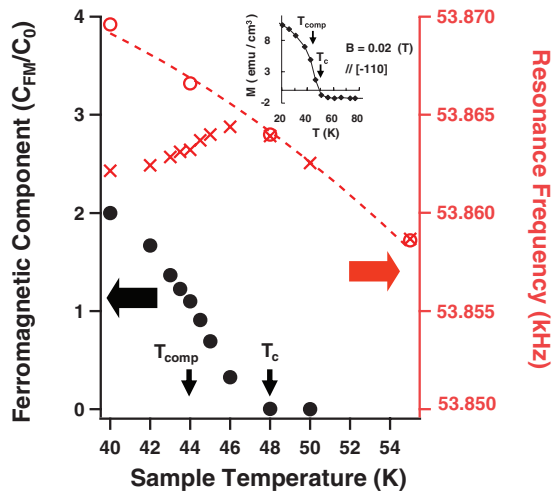


FIG. 4. (Color online) Relationship of the normalized ferromagnetic component of the PR as well as the resonance frequency as a function of temperature. Black dots show the temperature dependence of the ratio of the piezoresistive constants  $|C_{FM}/C_0|$ . Red crosses show the temperature dependence of the resonance frequency obtained by using Eqs. (3)–(6). Red circles show the temperature dependence of the resonance frequency in the presence of a sufficiently large out-of-plane magnetic field, i.e., when  $f_0$  saturates. The red dashed line shows the theoretical temperature dependence of the resonance frequency calculated by theory.<sup>29</sup> The inset shows the temperature dependence of magnetization, as measured with a SQUID magnetometer. (The diamagnetic response has not been subtracted.)

obtained using different mixing frequencies and different experimental setups, as well as different cantilever geometries. This strongly suggests that the delay time does not originate from the capacitive/inductive crosstalk of our experimental setup but solely from the response of the GaMnAs FMPR. The temperature dependence of the ferromagnetic coupling constant  $C_{FM}$  (black dots in Fig. 4) was obtained by fitting the data (Fig. 2) to Eqs. (3)–(6). Note that the value of  $C_{FM}$  increases monotonically below  $T_c$ . Such behavior of FMPR is similar to the temperature dependence of the magnetization of GaMnAs (inset in Fig. 4). The zero-magnetic-field resonance frequency (red crosses in Fig. 4) was also determined from the fitting. Cooling from a high temperature (55 K) initially causes it to increase. This behavior is well explained by the temperature dependence of the elastic constant<sup>28</sup> for the (100) plane of GaAs as follows:<sup>29</sup>

$$C_{ij}(T) = C_{ij}(0) \left\{ 1 - K_{ij} \times 3 \left( \frac{T}{T_D} \right)^4 \times \int_0^{T_D/T} x^3 (e^x - 1)^{-1} dx \right\}, \quad (10)$$

where  $C_{ij}(0)$  and  $K_{ij}$  are constants depending on material and  $T_D$  is Debye temperature. The temperature dependence of Young's module  $E$  can be calculated using Eq. (10) and  $C_{ij}(0)$ ,  $K_{ij}$ , and  $T_D$  from Refs. 29 and 30. The mechanical resonance frequency is proportional to  $E^{1/2}$ , following Hooke's law. The temperature dependence of the calculated resonance frequency  $f_0$  is shown in Fig. 4 (dashed line) and well coincides with our experimental data above  $T_c$ . Although this model is applicable

to Si,<sup>31</sup> III-V semiconductors,<sup>29</sup> or oxides,<sup>28</sup> it does neglect additional effects, e.g., magnetostriction, electrostriction, or thermal hysteresis. Nonetheless, here we assumed that those effects are of negligible strengths above  $T_c$ . However, below  $T_c$ , the resonance frequency decreases because of the appearance of ferromagnetic ordering. This softening is suppressed by the application of a magnetic field (red circles in Fig. 4), which breaks the spontaneous spin ordering, and the temperature dependence of the resonance frequency shows good agreement with the calculated temperature dependence of the elastic constant. These results indicate that the softening might originate from the spontaneous spin ordering.

Two mechanisms have been reported for the shift in the resonance frequency of GaMnAs: torque<sup>13</sup> and magnetoelasticity.<sup>14</sup> Since the softening is largest at zero magnetic field, torque is ruled out as a possibility. Thus, magnetoelasticity is responsible. However, a simple model of linear magnetostriction does not explain the phenomenon because the strain generated along the direction of the cantilever does not contribute to the frequency shift, in contrast to the case of a double clamped beam resonator.<sup>14,32</sup> A nonlinear elastic response or a higher-order magnetostriction effect could be the origin, but further investigations are required in order to clarify its influence.

Finally, we discuss the origin of the FMPR. Induced strain modulates the band structure of *n*-type GaAs, generating the nonferromagnetic PR component.<sup>3–5</sup> Similarly, in a GaAs two-dimensional hole system, PR has been observed due to the change in the heavy-hole valence band structure caused by applied strain.<sup>6</sup> Since the ferromagnetism of GaMnAs is known to be hole mediated, strain-induced deformation of the valence band structure might lead to the strain-induced perturbation of ferromagnetic spin ordering, which would then generate FMPR. The presence of strain causes or changes the splitting of heavy- and light-hole bands, leading to a hole concentration distribution between the two bands. The ferromagnetic ordering of GaMnAs is known to depend on the hole concentration,<sup>33</sup> indicating that strain can perturb ferromagnetic spin ordering. The time constant of  $\tau = 230 \pm 35$  ns is the response time in the PR of GaMnAs to the applied strain, but it is very long compared to other measurement results.<sup>17–19</sup> More detailed study, including the use of other samples or gated structures, is necessary to clarify the origin of this long delay time.

In conclusion, we studied the temperature and magnetic-field dependence of the PR of GaMnAs around  $T_c$ . We found that the PR has a ferromagnetic-induced component, which is caused by the strain-induced perturbation of the spontaneous spin ordering. This component was shown to have a response time of  $230 \pm 35$  ns with respect to induced strain.

#### ACKNOWLEDGMENTS

The authors thank Yoshiji Horikoshi for his encouragement throughout this work. They are also grateful to T. Fujisawa, T. Yamaguchi, H. Yamamoto, Y. Ishikawa, S. Kobayashi, K. Yanagisawa, S. Takeuchi, and H. Yoshitake for their help. This work was partly supported by a Grant-in-Aid for Scientific Research from the Japan Society for the Promotion of Science (Grants No. 20246064 and No. 23241046).

- <sup>1</sup>C. S. Smith, *Phys. Rev.* **94**, 42 (1954).
- <sup>2</sup>G. Dorda, *J. Appl. Phys.* **42**, 2053 (1971).
- <sup>3</sup>A. Sagar, *Phys. Rev.* **112**, 1533 (1958).
- <sup>4</sup>D. A. Aspnes and M. Cardona, *Phys. Rev. B* **17**, 741 (1978).
- <sup>5</sup>R. J. Sladek, *Phys. Rev.* **140**, A1345 (1965).
- <sup>6</sup>B. Habib, J. Shabani, E. P. De Poortere, M. Shayegan, and R. Winkler, *Appl. Phys. Lett.* **91**, 012107 (2007).
- <sup>7</sup>R. L. Parker and A. Krinsky, *J. Appl. Phys.* **34**, 2700 (1963).
- <sup>8</sup>C. J. Reilly and J. E. Sanchez, *J. Appl. Phys.* **85**, 1943 (1999).
- <sup>9</sup>H. Bhaskaran, M. Li, D. Garcia-Sanchez, P. Zhao, I. Takeuchi, and H. Tang, *Appl. Phys. Lett.* **98**, 013502 (2011).
- <sup>10</sup>M. Tortonese, R. C. Barrett, and C. F. Quate, *Appl. Phys. Lett.* **62**, 834 (1993).
- <sup>11</sup>H. Yamaguchi, Y. Hirayama, S. Miyashita, and S. Ishihara, *Appl. Phys. Lett.* **86**, 052106 (2005).
- <sup>12</sup>M. Li, H. X. Tang, and M. L. Roukes, *Nat. Nanotechnol.* **2**, 114 (2007).
- <sup>13</sup>J. G. E. Harris, D. D. Awschalom, F. Matsukura, H. Ohno, K. D. Maranowski, and A. C. Gossard, *Appl. Phys. Lett.* **75**, 1140 (1999).
- <sup>14</sup>S. C. Masmanidis, H. X. Tang, E. B. Myers, M. Li, K. De Greve, G. Vermeulen, W. Van Roy, and M. L. Roukes, *Phys. Rev. Lett.* **95**, 187206 (2005).
- <sup>15</sup>J. Honolka, S. Masmanidis, H. X. Tang, M. L. Roukes, and D. D. Awschalom, *J. Appl. Phys.* **97**, 063903 (2005).
- <sup>16</sup>M. Yamanouchi, D. Chiba, F. Matsukura, T. Dietl, and H. Ohno, *Phys. Rev. Lett.* **96**, 096601 (2006).
- <sup>17</sup>H. Munekata, *Physica E* **29**, 475 (2005).
- <sup>18</sup>A. V. Kimel, G. V. Astakhov, G. M. Schott, A. Kirilyuk, D. R. Yakovlev, G. Karczewski, W. Ossau, G. Schmidt, L. W. Molenkamp, and Th. Rasing, *Phys. Rev. Lett.* **92**, 237203 (2004).
- <sup>19</sup>Y. Hashimoto, S. Kobayashi, and H. Munekata, *Phys. Rev. Lett.* **100**, 067202 (2008).
- <sup>20</sup>Y. Horikoshi, M. Kawashima, and H. Yamaguchi, *Jpn. J. Appl. Phys., Part 2* **25**, L868 (1986).
- <sup>21</sup>M. Dobrowolska, K. Tivakornsasithorn, X. Liu, J. K. Furdyna, M. Berciu, K. M. Yu, and W. Walukiewicz, *Nat. Mater.* **11**, 444 (2012).
- <sup>22</sup>F. Matsukura, H. Ohno, A. Shen, and Y. Sugawara, *Phys. Rev. B* **57**, R2037 (1998).
- <sup>23</sup>K. Y. Wang, K. W. Edmonds, R. P. Campion, L. X. Zhao, C. T. Foxon, and B. L. Gallagher, *Phys. Rev. B* **72**, 085201 (2005).
- <sup>24</sup>H. Yamaguchi, Y. Tokura, S. Miyashita, and Y. Hirayama, *Phys. Rev. Lett.* **93**, 036603 (2004).
- <sup>25</sup>I. Bargatin, E. B. Myers, J. Arlett, B. Gudlewski, and M. L. Roukes, *Appl. Phys. Lett.* **86**, 133109 (2005).
- <sup>26</sup>In this Rapid Communication, we define the piezoresistance as  $\Pi = R\varepsilon\pi$ , where  $\varepsilon$  is the applied strain,  $R$  is the original resistance, and  $\pi$  is the piezoresistive gauge factor, which is just the change in net resistance induced by strain.
- <sup>27</sup>J. P. Den Hartog, in *Mechanical Vibrations* (Dover, New York, 1985), p. 47.
- <sup>28</sup>J. B. Wachtman, W. E. Tefft, D. G. Lam, and C. S. Apstein, *Phys. Rev.* **122**, 1754 (1961).
- <sup>29</sup>W. F. Hoyle and R. J. Sladek, *Phys. Rev. B* **11**, 2933 (1975).
- <sup>30</sup>T. B. Bateman, H. J. McSkimin, and J. M. Whelan, *J. Appl. Phys.* **30**, 544 (1959).
- <sup>31</sup>U. Gysin, S. Rast, P. Ruff, E. Meyer, D. W. Lee, P. Vettiger, and C. Gerber, *Phys. Rev. B* **69**, 045403 (2004).
- <sup>32</sup>H. Yamaguchi, K. Kato, Y. Nakai, K. Onomitsu, S. Warisawa, and S. Ishihara, *Appl. Phys. Lett.* **92**, 251913 (2008).
- <sup>33</sup>T. Dietl, H. Ohno, and F. Matsukura, *Phys. Rev. B* **63**, 195205 (2000).